jUMP

Joint Action: a stepping-stone for underwater noise monitoring in Portuguese water

Application of the acoustics models in the jUMP project

Autor	Alberto Azevedo e Beatriz Caetano
Data	26/05/2023
Tipo de documento	Público

Data	Versão	Alterações
10/12/2022	Draft	Alberto Azevedo e Beatriz Caetano
26/05/2023	Final	Alberto Azevedo e Beatriz Caetano

INDEX

INDEX 3
1 SUMÁRIO EXECUTIVO 4
2 EXECUTIVE SUMMARY 4
3 SELECTION OF THE ACOUSTICS MODELS 5
3.1 FACTORS OF CHOICE FOR THE MODELS 5
3.2 SELECTED ACOUSTIC MODELS 5
4 VALIDATION OF THE MODELS 6
4.1 BELLHOP 6
4.2 KRAKEN 7
5 APPLICATION THE MODELS 9
5.1 1º SNAPSHOT: AVEIRO SPRING 9
5.1.1 SIMULATION WITH COPERNICUS DATA: TRANSMISSION LOSS 10
5.1.2 SIMULATION WITH CTD DATA: TRANSMISSION LOSS 14
5.1.3 SIMULATION WITH COPERNICUS DATA: SOUND PRESSURE LEVEL 16
5.1.4 SIMULATION WITH CTD DATA: SOUND PRESSURE LEVEL 18
5.2 2º SNAPSHOT: AVEIRO AUTUMN 21
5.2.1 SIMULATION WITH COPERNICUS DATA: TRANSMISSION LOSS 21
5.2.2 SIMULATION WITH CTD DATA: TRANSMISSION LOSS 23
5.2.3 SIMULATION WITH COPERNICUS DATA: SOUND PRESSURE LEVEL 24
5.2.4 SIMULATION WITH CTD DATA: SOUND PRESSURE LEVEL 25
5.3 1º SNAPSHOT: ALGARVE SPRING 26
5.3.1 SIMULATION WITH COPERNICUS DATA: TRANSMISSION LOSS 27
5.3.2 SIMULATION WITH CTD DATA: TRANSMISSION LOSS 27
5.3.3 SIMULATION WITH COPERNICUS DATA: SOUND PRESSURE LEVEL 29
5.3.4 SIMULATION WITH CTD DATA: SOUND PRESSURE LEVEL 29
5.4 2º SNAPSHOT: ALGARVE AUTUMN 31
5.4.1 SIMULATION FOR TRANSMISSION LOSS 31
5.4.2 SIMULATION FOR SOUND PRESSURE LEVELS 33
6 CONCLUSIONS 34
7 REFERENCES 35
8 ANNEX I. ACRONYMS 35

1 SUMÁRIO EXECUTIVO

O principal objetivo do projeto jUMP é contribuir para a gestão sustentável do ruído subaquático e ajudar as autoridades nacionais a resolver os problemas do Descritor 11. Entre vários objetivos distintos, os modelos acústicos oceânicos são uma das ferramentas necessárias e utilizadas pela comunidade científica para estudar a propagação do som e as suas consequências no meio marinho. A modelação numérica pode simular cenários hipotéticos e avaliar a propagação sonora gerada por atividades humanas, como tráfego de navios ou mesmo a instalação de campos de geração de energia marinha (e.g. geradores eólicos ou oceanográficos), em águas oceânicas e costeiras. Além disso, essas ferramentas de modelação numérica podem aperfeiçoar o conhecimento sobre a propagação de som no ambiente marinho com uma fração muito reduzida dos custos normais de campanhas de campo e medições in situ.

Este relatório tem como objetivo apresentar os resultados das simulações de decaimento da pressão acústica (Transmission Loss - TL) e pressão acústica (Sound Pressure Level - SPL) realizadas com os modelos BELLHOP e KRAKEN, implementados no portal de modelação (http://jump-app.lnec.pt/index/), utilizando dados de modelação do Copernicus. Foram efetuadas várias simulações para cada uma das campanhas realizadas durante o projeto, em Aveiro durante a Primavera e o Outono, e no Algarve durante a Primavera e Outono.

2 EXECUTIVE SUMMARY

The primary goal of the jUMP project is to contribute to the sustainable management of underwater noise and assist national authorities in addressing issues related to Descriptor 11. Among the various objectives, ocean acoustic models serve as essential tools that the scientific community utilizes to investigate sound propagation and its impacts on the marine environment. Numerical modeling enables the simulation of hypothetical scenarios and the assessment of sound propagation caused by human activities, such as ship traffic or the establishment of marine energy generation fields (e.g., wind or oceanographic generators), in both oceanic and coastal waters. Moreover, these numerical modeling tools significantly enhance our understanding of sound propagation in the marine environment at a fraction of the usual costs associated with field campaigns and in situ measurements.

This report aims to present the outcomes of simulations conducted using the BELLHOP and KRAKEN models, integrated into the modeling portal (http://jump-app.lnec.pt/index/), and utilizing Copernicus oceanographic modeling data. The simulations encompassed multiple scenarios for each campaign conducted during the project, including those in Aveiro during spring and autumn, and in the Algarve during spring and autumn. Furthermore, the simulations specifically focused on the decay of acoustic pressure (Transmission Loss - TL) and the measurement of acoustic pressure (Sound Pressure Level - SPL).

3 SELECTION OF THE ACOUSTICS MODELS

3.1 Factors of choice for the models

The purpose of the acoustic models is to model the noise created by human activity, focusing on the noise generated by shipping and by fields of wind generators. Consequently, the models must be adequate for low frequencies ($< 1kHz$). Therefore, all methods can be used except for the ray method, which is more suitable for high frequencies. However, two models will be used to increase the applicability domain, one for low frequencies and the other for higher frequencies.

Regarding implementing the domain factors, the model must be range-dependent to simulate the environment most completely and realistically possible. Regarding depth, it must be able to be applied in shallow and deep-water situations. If there is a parallelized version of the model, preference is given to that version to take advantage of the computational power available, improving computing time.

The last criterion is that the software must be freely accessible. If this criterion were not imposed, there would have been a wide variety of models to choose from that are synthesized in Etter, 2018. However, considering this criterion, the models that can be considered are those available at OALIB.

3.2 Selected acoustic models

At OALIB, several available models are grouped according to their method. In addition to the various models, there is also a Toolbox called AcTUP v2.2L (Acoustic Toolbox User interface and Postprocessor), which is the most recent version. The toolbox includes BELLHOP, KRAKEN, KRAKENC, RAMGEO, RAMSGEO, and SCOOTER (Maggi et al., 2006).

The interface of the toolbox was developed for Matlab and provides output files with the results, along with several graphical representation tools (Duncan et al., 2006). Additionally, there is an interface available for the Python toolbox developed by Hunter Akins at UCSD, and Python scripts for reading the output files created by Orlando Rodriguez at the University of Algarve.

Considering all the criteria and the models available for low-frequency situations, the implemented model will be BELLHOP. For lower frequencies, the pre-selected models were RAM and KRAKEN. After testing, KRAKEN was chosen since the results of both models are similar (Sertlek et al., 2013 & Küsel et al., 2019). Moreover, KRAKEN has input files similar to those of BELLHOP, which facilitates the implementation of both models. Therefore, the toolbox that incorporates both models will be used, with its implementation in Python.

4 VALIDATION OF THE MODELS

4.1 BELLHOP

For the validation of the models, the example of Munk's profile presented in the manuals of the respective models is replicated (Porter, 2001 & Porter, 2011). This example also illustrates the typical behaviour of sound propagation in deep waters.

Munk's profile provides an analytical expression (Equation 4.1) that offers a good approximation for the variation of sound speed with depth in deep-water environments. Furthermore, this expression is valid in the vicinity of a deep sound channel (Etter, 2018).

$$c(z) = c_1[1 + \varepsilon(\eta + e^{-\eta} - 1)]$$
$$\eta = \frac{2(z - z_1)}{B} \qquad \varepsilon = \frac{B\gamma_a}{2} \tag{4.1}$$

where $c(z)$ is the speed of sound as a function of depth, c_1 is the minimum speed of sound in the deep sound channel, z_1 the depth where the speed of sound is minimum, η the relative distance to the sound channel (parameter dimensionless), B the depth scale, ε the perturbation coefficient, and γ_a the sound velocity gradient for the adiabatic ocean. Typical values defined by Munk (1974) are $c_1 = 1500\ ms^{-1}$, $B = 1.3\ km$, $z_1 = 1.3\ km$, $\gamma_a = 1.14 \times 10^{-2}\ km^{-1}$ e $\varepsilon = 7.4 \times 10^{-3}$ (Etter, 2018).

For numerical simulation, a signal with a frequency of $50\ Hz$ is considered. The source is located at a depth of $1000\ m$, and the ocean depth is $5000\ m$. The maximum distance for the simulation is set at $100000\ m$. The density of seawater is $1000\ kg/m^3$. In the solid layer that constitutes the ocean floor, the sound speed remains constant at $1600\ m/s$. The density of the solid layer is $1800\ kg/m^3$, and the acoustic attenuation coefficient is 0,8 dB per wavelength ($\alpha(dB\ \lambda^{-1})$, where $\alpha(dBm^{-1}\ )$ is the attenuation coefficient per meter). The illustrative scheme of the configuration of this test is in Figure 4.1.

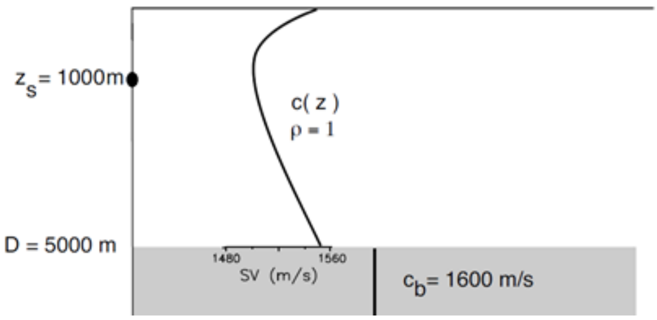

Figure 4.1: Illustrative scheme of Munk's test, adapted from (Porter, 2001) where $c(z)$ is the profile of the speed of sound in the water column, z_s is the depth of the source, ρ is the density gcm^{-3}), D is the depth of the ocean floor and c_b is the speed in the ocean floor.

Figure 4.2 displays the propagation loss profile taken from the BELLHOP manual (Porter, 2011) on the left, and the corresponding example obtained by running the BELLHOP model on the right. It is evident that the pattern and values obtained in the model execution closely resemble those of the reference figure. Therefore, the installed version of the model has been validated and can be effectively utilized in future tests.

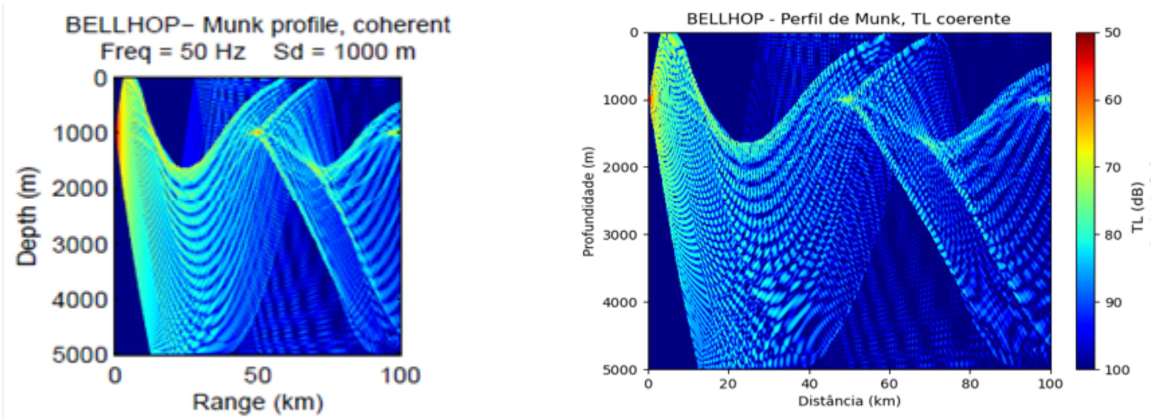

Figure 4.2: First (figure on the left) TL profile taken from the BELLHOP manual (Porter, 2011), second (figure on the right) TL profile obtained through the execution of the BELLHOP model referring to Munk's test ($f = 50Hz$).

Although this model is typically indicated for high frequencies, in this test, it is considered a low frequency due to the need to maintain the parameters specified in the manuals (Porter, 2001 & 2011). This provides an opportunity to assess the model's performance beyond its usual domain of applicability.

The rays propagate in depth until they reach the turning depth, which is the depth at which the speed of sound equals the maximum encountered by the ray. Once the turning depth is reached, the rays propagate towards the surface, eventually converging at the depth of the source, creating a convergence zone with high acoustic pressure (Abraham, 2019).

In situations where the ocean depth is significant enough that the speed of sound near the bottom is higher than at the surface, as in the example under study, certain rays will not interact with the ocean bottom or free surface. This occurs because the depth of the simulation domain exceeds the depth at which the velocity matches the surface velocity (critical depth) (Abraham, 2019).

4.2 KRAKEN

The same procedure was then carried out for the KRAKEN model, using the same parameters. On the left, Figure 4.3 displays the propagation loss profile of this model, taken from Porter (2011), while on the right is the example obtained by running the installed version of the KRAKEN model. Upon comparing the two TL profiles, it is evident that the values and characteristics align, affirming that the installed version of the KRAKEN model can be reliably employed in subsequent tests.

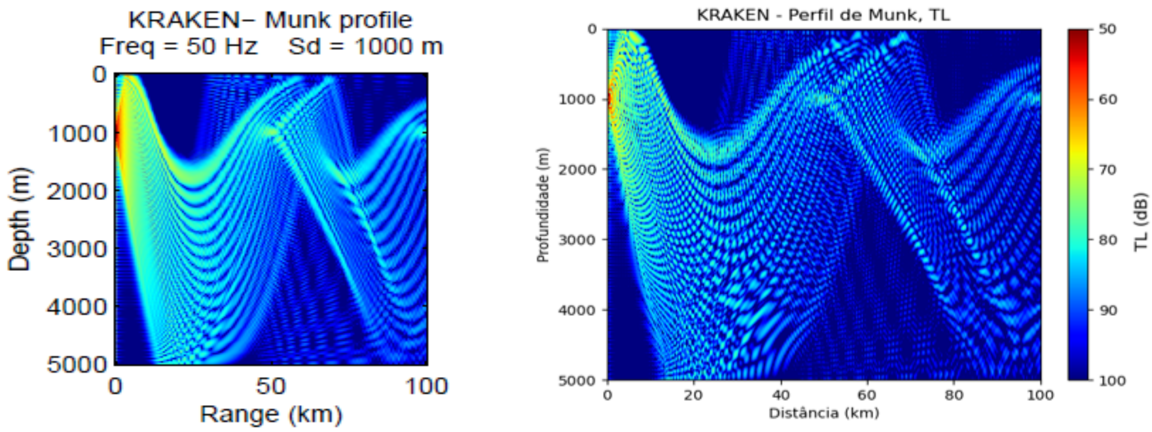

Figure 4.3: The first TL profile (figure on the left) represents the KRAKEN model obtained from the BELLHOP manual (Porter, 2011). The second TL profile (figure on the right) illustrates the results obtained by executing the KRAKEN model for the Munk test with a frequency of $50\ Hz$.

As the source is positioned near the depth where the speed of sound reaches its minimum ($1000\ m$), the tested case exemplifies the phenomenon of acoustic propagation in the deep sound channel, utilizing the Munk profile for the speed of sound. It is observed that rays with ascending or descending trajectories are refracted towards the depth of the source.

The example being studied also illustrates a reliable acoustic path characterized by a dominant propagation route. This is attributed to lower propagation loss and the existence of a pathway that connects deeper waters with shallower waters. In practical terms, this means that a receiver can be placed at a depth where the speed of sound does not exceed the surface speed. Consequently, long-distance propagation to the surface becomes achievable without significant interactions with the seabed (Thompson, 2009).

5 APPLICATION THE MODELS

During the project, four snapshots were taken to gather acoustic data, two in Aveiro and one in Algarve (Ria Formosa). For each campaign, acoustic modeling was conducted, which involved obtaining sound profiles for the study area, geo-acoustic characteristics of the ocean floor, and the position and frequency of the sound source. In order to calculate the sound profiles, acoustic simulations were carried out using Copernicus data prior to the snapshots, and then using data collected by the CTD.

5.1 1º Snapshot: Aveiro Spring

The first snapshot occurred on March 16th, 2021 in Aveiro. Three hydrophones were deployed, and a total of four measurements were taken at distances of $1\ km$, $3\ km$, $5\ km$, and at a point equidistant from the three hydrophones. The configuration is depicted in Figure 5.1.

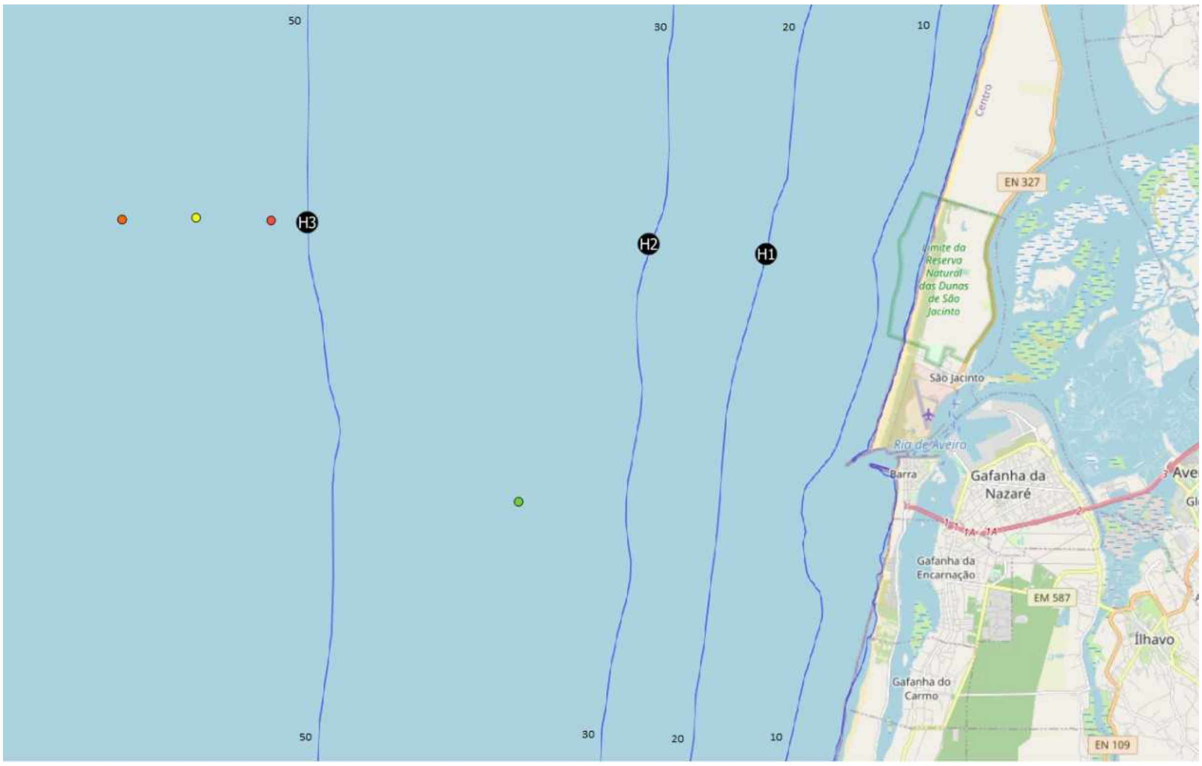

Figure 5.1: Configuration of the hydrophones and receptors for the Aveiro campaign.

In the environmental file of the models, various parameters are defined, including sound velocity profiles, domain characteristics, geo-acoustic parameters of the bottom, frequency, and source depth. The sound velocity profiles were computed using the formulation proposed by Leroy et al. (2008) (Equation 5.1), which considers temperature, salinity, and depth data.

$$c\ (S,T,P) = 1402.5 + 5T - 5.44 \times 10^{-2}T^{-2} + 2.1 \times 10^{-4}T^{3} + 1.33S - 1.23 \times 10^{-2}ST + 8.7 \times 10^{-5}ST^{2} + 1.56 \times 10^{-2}Z + 2.55 \times 10^{-7}Z^{2} - 7.3 \times 10^{-12}Z^{3} + 1.2 \times 10^{-6}Z(\Phi - 45) - 9.5 \times 10^{-13}TZ^{3} + 3 \times 10^{-7}T^{2}Z + 1.43 \times 10^{-5}SZ \quad (5.1)$$

The stratification parameters, including temperature, salinity, and depth, were obtained from CTD data collected during the campaigns. Alternatively, the Atlantic-Iberian Biscay Irish-Ocean Physics Analysis and Forecast (IBI_ANALYSISFORECAST_PHY_005_001) database from Copernicus Marine Services was utilized, using daily mean values (available at: https://resources.marine.copernicus.eu/product-detail/IBI_ANALYSISFORECAST_PHY_005_001/INFORMATION).

To determine the geo-acoustic parameters of the bottom, the geological composition of the seafloor needed to be defined. Two databases were consulted for this purpose: dbSEABED from the University of Colorado (accessible at: https://instaar.colorado.edu/~jenkinsc/dbseabed/) and the EMODnet broad-scale seabed habitat map for Europe (EUSeaMap) provided by the European Marine Observation and Data Network (EMODnet; available at: https://www.emodnet-seabedhabitats.eu/about/euseamap-broad-scale-maps/). The data obtained from these databases indicated that the study area predominantly consists of sandy bottoms. Thus, the bottom was characterized by a velocity of $1650\ m/s$, density of $1900\ kg/m^3$, and attenuation of 0,8 dB/λ (Etter, 2018).

In the case of the BELLHOP model, it was possible to define a bathymetry file by utilizing the geographic positions of the sound source and receiver. The bathymetric model of the study area was obtained from the Portuguese Hydrographic Institute through the EMODnet-bathymetry portal (available at: https://www.emodnet-bathymetry.eu).

5.1.1 Simulation with Copernicus data: Transmission Loss

Using Equation 5.1 and the temperature, salinity, and depth profiles from Copernicus, the sound speed profiles were calculated, and the results are depicted in Figure 5.2. These profiles were utilized for the simulations of the $1\ km$, $3\ km$, and $5\ km$ projections. Since there are three projections, three numerical simulations were conducted. In the $5\ km$ simulation, all nine sound speed profiles were incorporated. In the $3\ km$ simulation, profiles up to $16\ km$ were included, while in the $1\ km$ projection, profiles up to $14\ km$ were utilized.

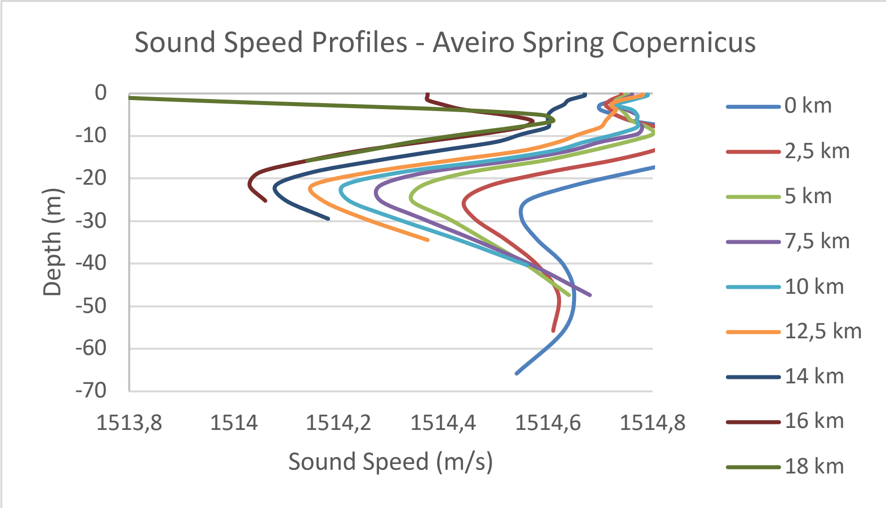

Figure 5.2: Sound speed profiles calculated from the Copernicus data.

In this campaign, the sound source was positioned at a depth of $10\ m$, and frequencies of $63\ Hz$, $125\ Hz$, $250\ Hz$, $500\ Hz$, $2\ kHz$, and $10\ kHz$ were emitted. The KRAKEN model was employed for frequencies of $63\ Hz$, $125\ Hz$, $250\ Hz$, while BELLHOP was used for the higher frequencies, as it is better suited for the high-frequency range. Both models calculate the propagation loss and generate profiles along the section, as depicted in Figure 5.3.

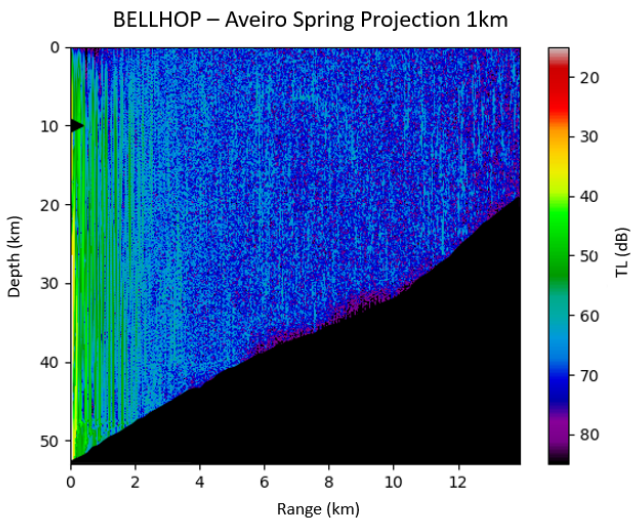

Figure 5.3: Transmission loss for the Aveiro campaign.

To compare the data obtained by the hydrophones in the campaigns with the results obtained by the models, the average transmission loss (TL) values were calculated. This was done by considering the TL profiles of the three hydrophones for each frequency and taking into account the different projections. The resulting average TL values are presented in Figure 5.4.

Firstly, the average TL value for each hydrophone's position was determined. This was done by calculating the average of the TL values within a radius of $50\ m$ from the hydrophone's location. Subsequently, an overall average was calculated by considering the values from the three simulations. For example, the TL value in H3 at a frequency of $63\ Hz$ (Figure 5.4) represents the average of the TL values for H3 at a frequency of $63\ Hz$ from the three simulations ($1\ km, 3\ km, 5\ km$).

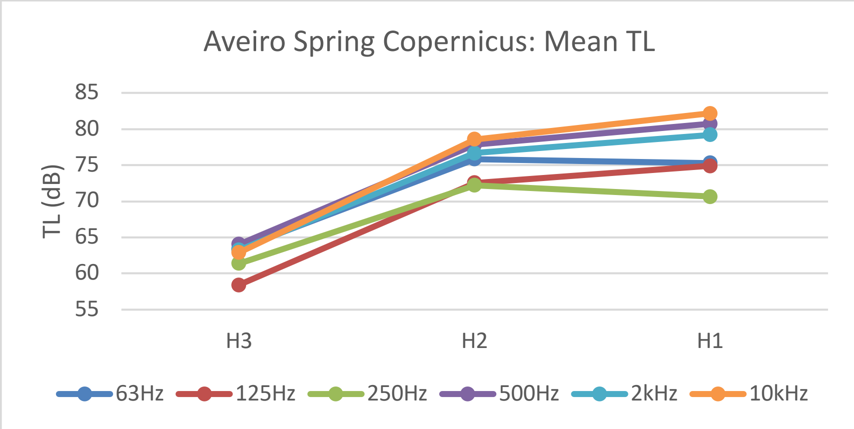

Figure 5.4: Mean transmission loss graph for the three projections, each point representing a frequency with Copernicus data for the snapshots carried out in Aveiro in spring.

The TL values increase for projections farther away from the sound source. This is because the distance between the source and the sound receiver is greater, resulting in higher signal losses. Table 1 presents the mean TL values as shown in Figure 5.4. The average TL value for the first snapshot in Aveiro using Copernicus data is $\mathbf{71,6\ dB}$.

Table 1: Mean TL values for each frequency in every hydrophone location, using Copernicus data.

	H3	H2	H1
63Hz	63,4	75,8	75,3
125Hz	58,4	72,6	74,9
250Hz	61,4	72,2	70,7
500Hz	64,0	77,8	80,7
2kHz	63,2	76,7	79,2
10kHz	62,9	78,6	82,2

Three simulations were conducted using the equidistant point as the source (indicated by the green dot on the map), with each simulation focusing on a specific hydrophone. Figure 5.5 displays the speed of sound profiles for all simulations, considering only the profiles relevant to each hydrophone in the respective simulation.

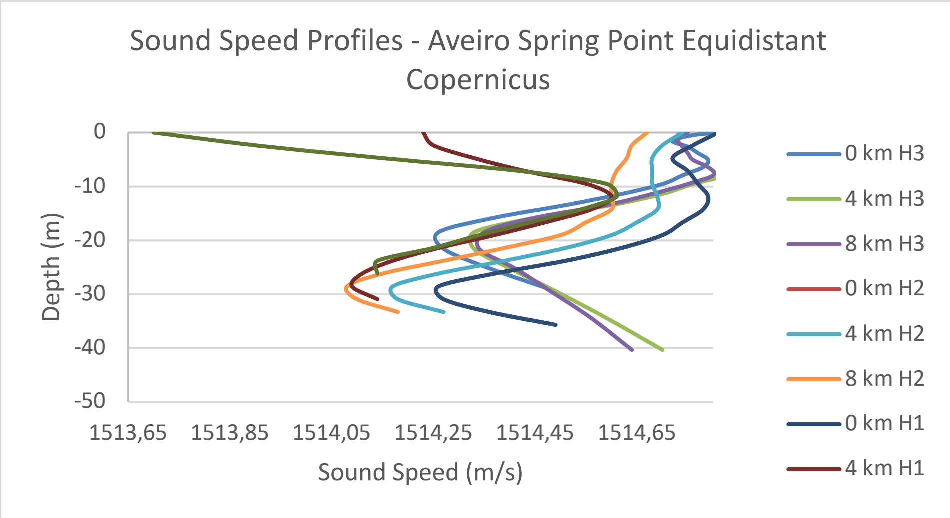

Figure 5.5: Sound speed profiles calculated from the Copernicus data.

Figure 5.6 presents the TL results of the three simulations. It is evident that the TL values for H1 and H2 are similar, indicating comparable results. In contrast, the TL values for H3 are higher, suggesting a distinct acoustic behaviour. This difference can be attributed to the fact that H1 and H2 are located in close proximity to each other and share similar topographic characteristics, whereas H3 exhibits different acoustic characteristics due to its distinct position.

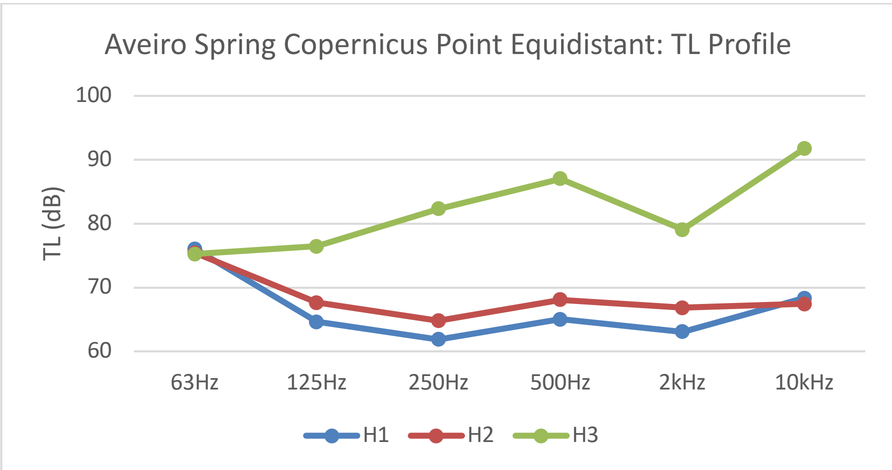

Figure 5.6: Mean transmission loss graph for the point equidistant simulation with Copernicus data for the snapshots carried out in Aveiro in spring.

In Table 2, the average TL values depicted in Figure 5.6 are presented. The average TL value for the first snapshot in Aveiro using Copernicus data for the equidistant point is $\mathbf{70,6\ dB}$.

Table 2: Mean TL values for each frequency in every hydrophone location, using Copernicus data for the equidistant point.

	H3	H2	H1
63Hz	75,2	75,4	76,1
125Hz	76,4	67,6	64,6
250Hz	82,3	64,8	61,9
500Hz	87,0	68,1	65,0
2kHz	79,1	66,8	63,0
10kHz	91,7	67,4	68,3

5.1.2 Simulation with CTD data: Transmission Loss

During the campaign, multiple CTD profiles were conducted, and the acquired data were utilized to conduct acoustic simulations using these sound speed profiles (Figure 5.7). The other parameters remained unchanged. Similar to previous simulations, the 5 km projection incorporated all six sound speed profiles, the 3 km simulation incorporated profiles up to 16 km, and the 1 km projection used profiles up to 14 km.

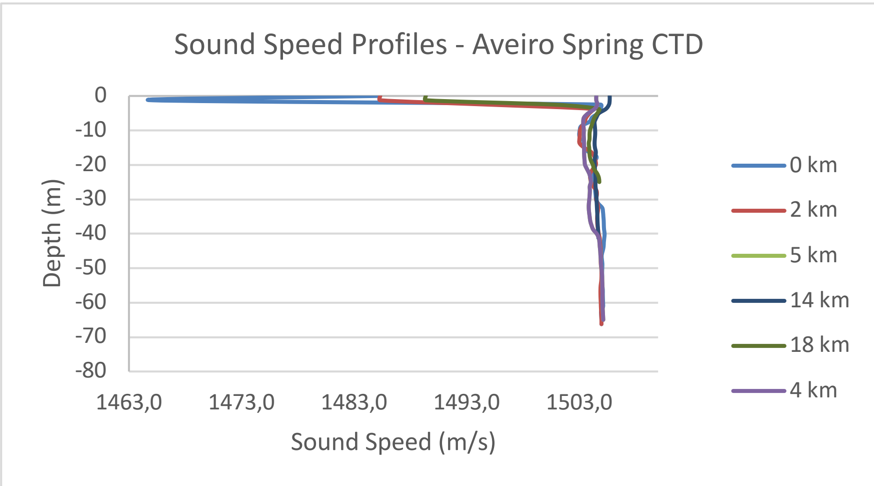

Figure 5.7: Sound speed profiles calculated from the CTD data.

The Figure 5.8 shows the average TL considering the three projections using the same method described in section 5.1.1, using CTD data. Like the simulations with Copernicus data, TL values increase with distance from the source and fall within the same range of values.

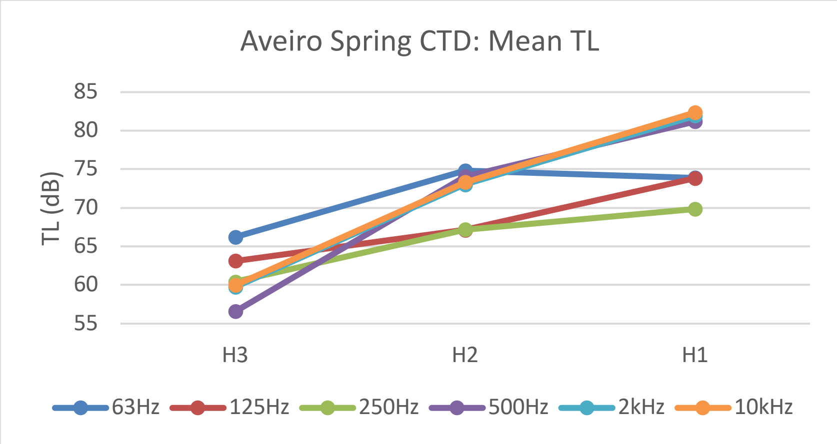

Figure 5.8: Mean transmission loss graph for the three projections, where each point represents a frequency, using CTD data for the snapshots conducted in Aveiro during spring.

In Table 3, the values of mean TL illustrated in Figure 5.8 are represented. The average TL value for the first snapshot of Aveiro using CTD data is 69,9 dB. Although TL values are not identical between Copernicus and CTD simulations, the average value is very close.

Table 3: Mean TL values for each frequency in every hydrophone location, using CTD data.

	H3	H2	H1
63Hz	66,2	74,8	73,9
125Hz	63,1	67,1	73,9
250Hz	60,4	67,2	69,9
500Hz	56,6	74,0	81,2
2kHz	59,8	73,0	81,9
10kHz	60,0	73,3	82,4

Then simulations were performed for the equidistant point using the sound velocity profiles shown in Figure 5.9, which were obtained through CTD data. In each simulation, a sound profile is used at the sound source (0 km) and the corresponding hydrophone (8 km).

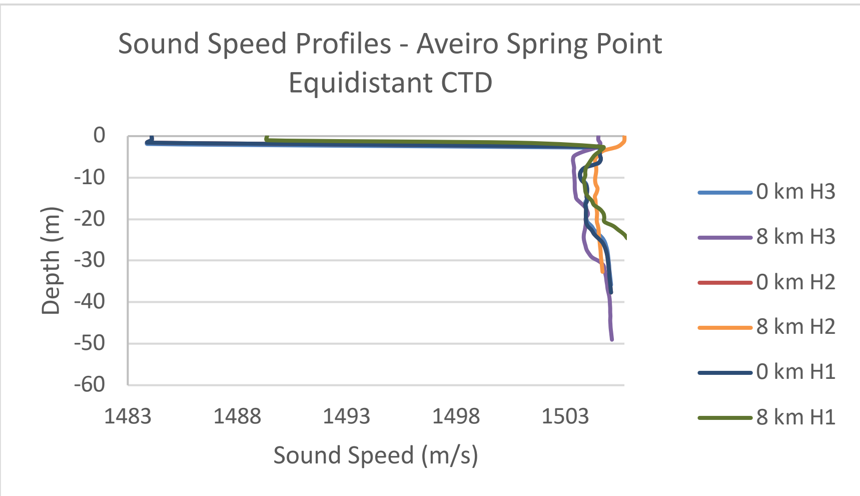

Figure 5.9: Sound speed profiles calculated from the CTD data.

In Figure 5.10, TL values are represented. As can be observed, the results are similar to the simulations using Copernicus data, although they are slightly higher, but still in the same order of magnitude. The largest discrepancy between H3 and the other hydrophones is also maintained.

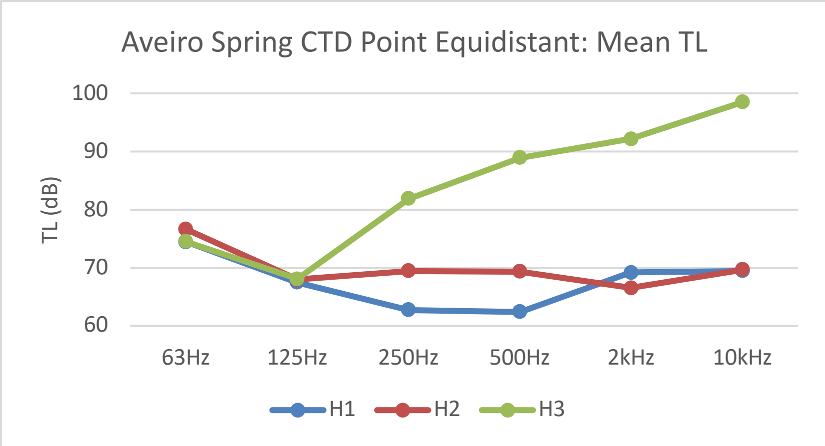

Figure 5.10: Mean transmission loss graph for the point equidistant simulation with CTD data for the snapshots carried out in Aveiro in spring.

In Table 4, the values of mean TL illustrated in Figure 5.10 are represented, and the average TL value for the first snapshot of Aveiro using CTD data for the equidistant point is $\mathbf{73,9\ dB}$. It is worth noting that the average value is higher in simulations with CTD data compared to those using Copernicus data.

Table 4: Mean TL values for each frequency in every hydrophone location, using CTD data for the equidistant point.

	H3	H2	H1
63Hz	74,5	76,6	74,5
125Hz	68,1	68,0	67,5
250Hz	81,9	69,5	62,7
500Hz	88,9	69,3	62,4
2kHz	92,2	66,5	69,2
10kHz	98,5	69,7	69,4

5.1.3 Simulation with Copernicus data: Sound Pressure Level

Sound pressure level (SPL) describes the intensity of sound. Based on the acoustic pressure data from the previous simulations, SPL was calculated using the following method:

$$SPL = 10\ log_{10} \frac{P^2}{P_0^2} \tag{5.2}$$

The reference value for pressure (P_0) in water is 1 μPa, and SPL is expressed in units of decibels relative to 1 μPa, or $dB\ re\ 1\ \mu Pa$. The average SPL values for simulations with Copernicus data are shown in Figure 5.11. The process described in section 5.2.1 was also used to calculate the average SPL values.

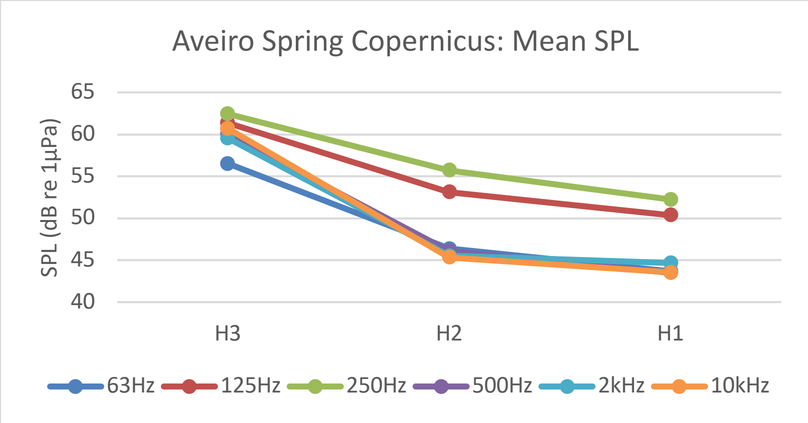

Figure 5.11: Mean sound pressure level graph for the three projections, each point representing a frequency with Copernicus data for the snapshots carried out in Aveiro in spring.

Table 5 presents the SPL values from Figure 5.11, and the average SPL value for Aveiro using Copernicus data is 51,7 $dB\ re\ 1\mu Pa$. Unlike TL, which increases with distance from the source due to the increasing loss of the acoustic signal, SPL exhibits the opposite behaviour. In proximity to the source, the acoustic pressure is higher, resulting in higher SPL values. As the distance increases, the acoustic pressure decreases, leading to a decrease in SPL.

Table 5: Mean SPL values for each frequency in every hydrophone location, using Copernicus data.

	H3	H2	H1
63Hz	56,5	46,4	43,7
125Hz	61,4	53,1	50,4
250Hz	62,4	55,7	52,2
500Hz	60,0	46,1	43,5
2kHz	59,5	45,5	44,7
10kHz	60,7	45,3	43,6

The SPL values were calculated for the equidistant point using Equation 5.2, and the results are shown in Figure 5.12. As the frequency increases, the differences between H3 and the other hydrophones also become more pronounced. Consequently, the greatest similarity can be observed between H1 and H2.

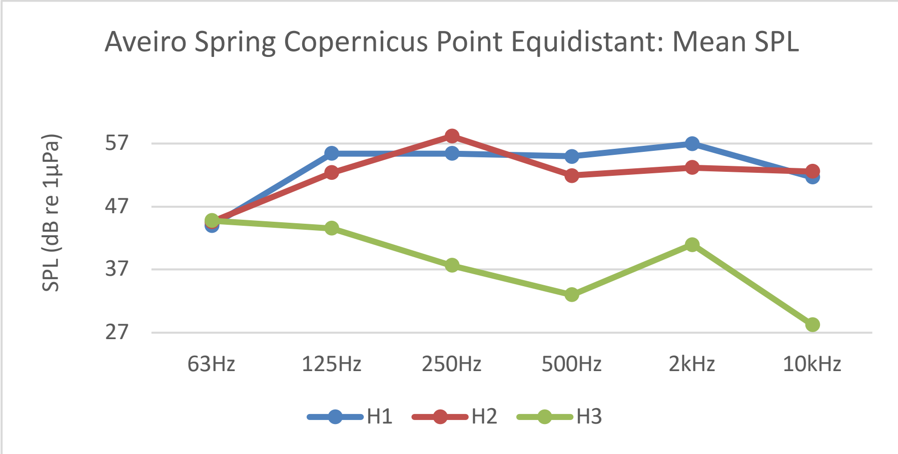

Figure 5.12: Mean sound pressure level graph for the point equidistant simulation with Copernicus data for the snapshots carried out in Aveiro in spring.

Table 6 shows the values presented in Figure 5.12. The average SPL value for the first snapshot in Aveiro, using Copernicus data for the equidistant point, is $47{,}5\ dB\ re\ 1\mu Pa$.

Table 6: Mean SPL values for each frequency in every hydrophone location, using Copernicus data for the equidistant point.

	H3	H2	H1
63Hz	44,8	44,6	44,0
125Hz	43,6	52,4	55,4
250Hz	37,7	58,2	55,4
500Hz	33,0	51,9	55,0
2kHz	41,0	53,2	57,0
10kHz	28,3	52,6	51,7

5.1.4 Simulation with CTD data: Sound Pressure Level

Using Equation 5.2 and the acoustic pressure values obtained from the simulations based on the CTD data, the average SPL was determined and is represented in Figure 5.13. Similar to earlier observations, SPL values decrease with increasing distance from the sound source (H3 hydrophone being closer to the source).

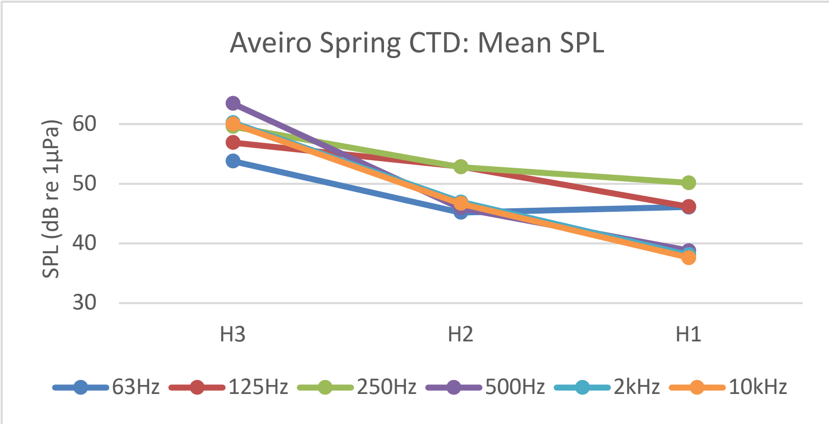

Figure 5.13: Mean sound pressure level graph for the three projections, each point representing a frequency with CTD data for the snapshots carried out in Aveiro in spring.

Table 7 presents the values shown in Figure 5.13. Based on the CTD data from Aveiro, the average SPL is $\mathbf{50,1\ dB\ re\ 1\mu Pa}$, which agrees with the results obtained using the Copernicus data.

Table 7: Mean SPL values for each frequency in every hydrophone location, using CTD.

	H3	H2	H1
63Hz	53,8	45,2	46,1
125Hz	56,9	52,9	46,2
250Hz	59,6	52,8	50,1
500Hz	63,4	46,0	38,8
2kHz	60,2	47,0	38,1
10kHz	60,0	46,7	37,6

Figure 5.14 depicts the mean SPL for the simulations conducted at the equidistant point, and the results are like those obtained with the Copernicus data. The average SPL value for the first snapshot of Aveiro using Copernicus data for the equidistant point is $48{,}3\ dB\ re\ 1\mu Pa$.

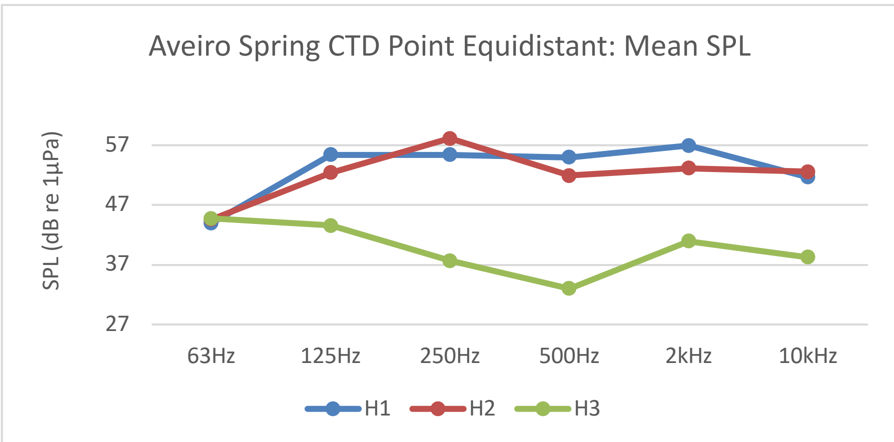

Figure 5.14: Mean sound pressure level graph for the point equidistant simulation with CTD data for the snapshots carried out in Aveiro in spring.

Table 8 presents the values shown in Figure 5.14. The average SPL value for the first snapshot of Aveiro using Copernicus data for the equidistant point is $\mathbf{48,3\ dB\ re\ 1\mu Pa}$.

Table 8: Mean SPL values for each frequency in every hydrophone location, using Copernicus data for the equidistant point.

	H3	H2	H1
63Hz	43,9	44,6	44,8
125Hz	55,4	52,4	43,6
250Hz	55,4	58,1	37,7
500Hz	55,0	51,9	33,0
2kHz	57,0	53,2	40,9
10kHz	51,7	52,6	28,3

5.2 2º Snapshot: Aveiro Autumn

The second snapshot took place on July 2nd, 2021 in Aveiro, in the same area as the first snapshot. Three hydrophones were used, and a total of three projections were made at $100\ m, 250\ m, and\ 500\ m$. The scheme is illustrated in Figure 5.15.

Figure 5.15: Configuration of the hydrophones and receptors for the second Aveiro campaign.

5.2.1 Simulation with Copernicus data: Transmission Loss

Equation 5.1 and the temperature, salinity, and depth profiles from Copernicus were used to calculate the sound speed profile shown in Figure 5.16. In contrast to the first snapshot, where multiple velocity profiles were available throughout the domain, in this campaign, only one profile is considered due to the spatial resolution limitations of the database, which provides data for a single point.

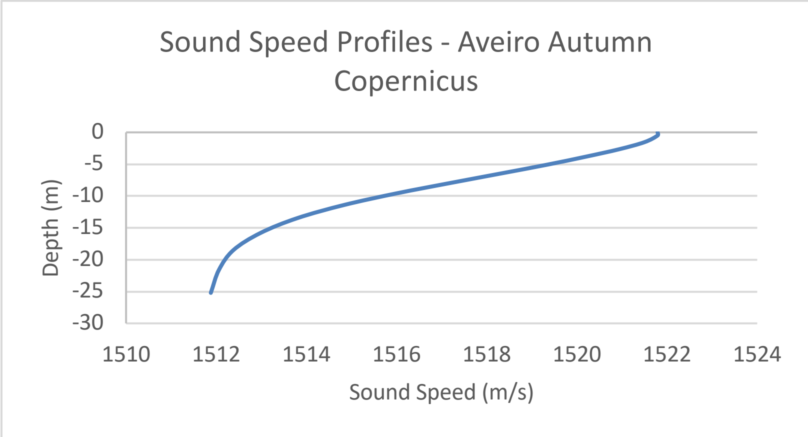

Figure 5.16: Average sound velocity (m/s) profile, for the snapshots carried out in Aveiro in autumn with Copernicus data.

Using the same method as in the spring simulations, the transmission loss was calculated, and its profile is shown in Figure 5.17. The average TL value is recorded as 55,1 dB, with results ranging from 47,4 dB to 61,01 dB. Since the hydrophones are positioned relatively close to each other during this operation, there are significant similarities among the TL values obtained.

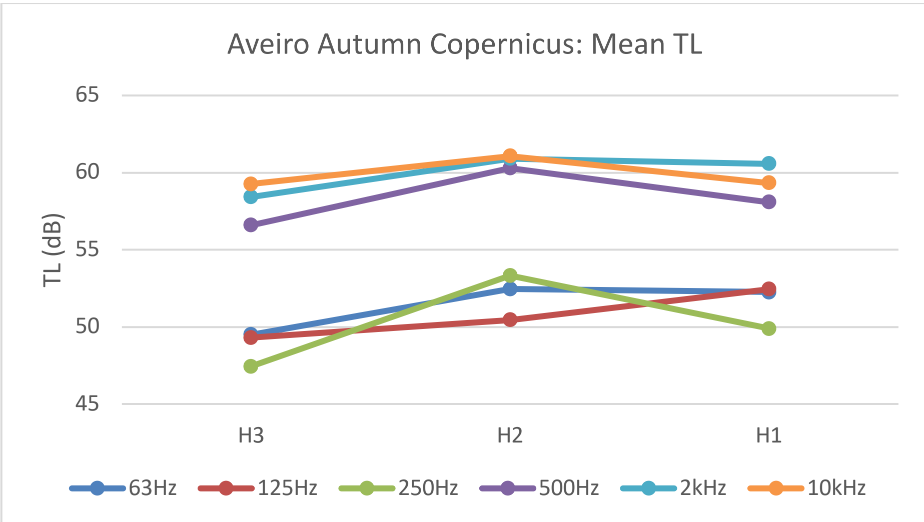

Figure 5.17: Mean transmission loss graph for the three projections, each point representing a frequency with Copernicus data for the snapshots carried out in Aveiro in autumn.

In Table 9 are represented the values of mean TL illustrated in Figure 5.17.

Table 9: Mean TL values for each frequency in every hydrophone location, using Copernicus data.

	H3	H2	H1
63Hz	49,5	52,5	52,2
125Hz	49,4	50,5	52,4
250Hz	47,4	53,3	49,9
500Hz	56,6	60,3	58,1
2kHz	58,4	60,9	60,6
10kHz	59,3	61,1	59,3

5.2.2 Simulation with CTD data: Transmission Loss

By utilizing the CTD information collected during the expedition, various sound speed profiles were established. All six sound speed profiles were considered for simulating a projection at $500\ m$. Up to a depth of $810\ m$, all the profiles were incorporated in a simulation at $100\ m$. For the projection at $250\ m$, only the profiles up to $500\ m$ were utilized.

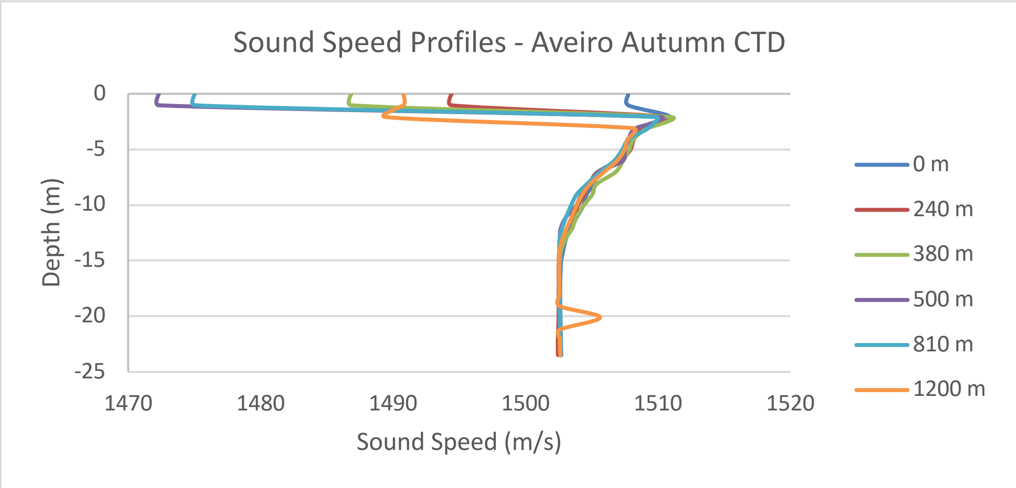

Figure 5.18: Sound speed profiles calculated from the CTD data.

The TL values obtained are depicted in Figure 5.19, with an average value of $55{,}8\ dB$ when all frequencies are considered. Similar to the results obtained from Copernicus data, there is a variance between low and high frequency TL values, where the highest TL is observed in the high frequency range.

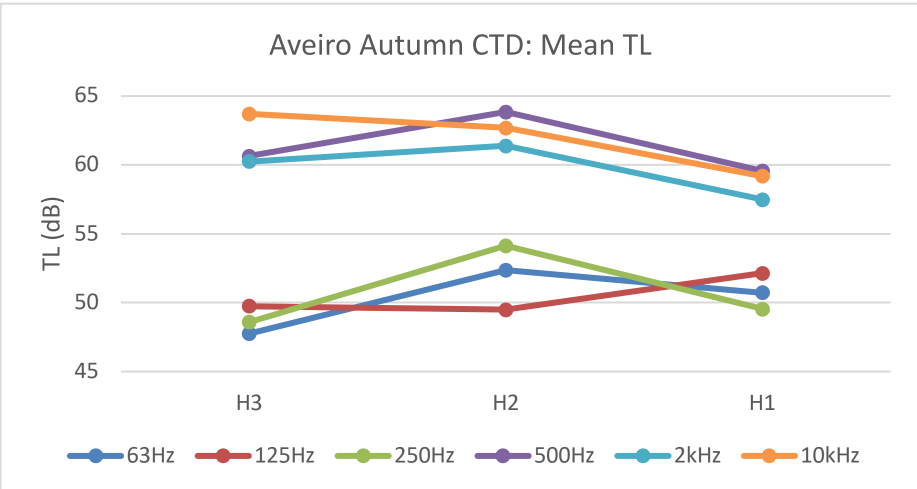

Figure 5.19: Mean transmission loss graph for the three projections, each point representing a frequency with Copernicus data for the snapshots carried out in Aveiro in autumn.

By comparing both simulations, it can be observed that the average values as well as the values in each frequency range are quite similar. Table 10 displays the mean TL values depicted in Figure 5.19.

Table 10: Mean TL values for each frequency in every hydrophone location, using CTD data for the equidistant point.

	H3	H2	H1
63Hz	47,8	52,4	50,7
125Hz	49,7	49,5	52,1
250Hz	48,6	54,1	49,5
500Hz	60,6	63,9	59,6
2kHz	60,2	61,4	57,5
10kHz	63,7	62,7	59,2

5.2.3 Simulation with Copernicus data: Sound Pressure Level

Based on Equation 5.2 and the procedure described in section 5.1.3, the SPL values were determined for the simulations with Copernicus data (Figure 5.20). It can be observed that the SPL values decrease with the distance from the source. The average value is 67,6 $dB\ re\ 1\mu Pa$, with results ranging between 57,1 and 74,8 $dB\ re\ 1\mu Pa$.

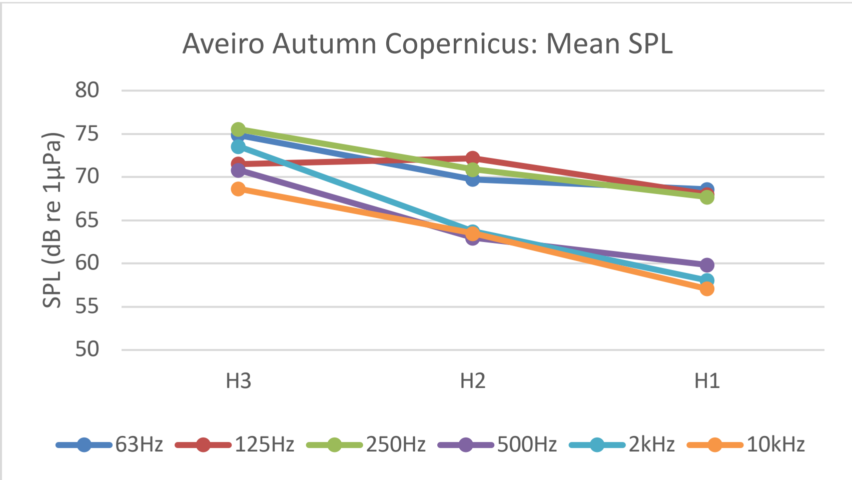

Figure 5.20: Mean sound pressure level graph for the three projections, each point representing a frequency with Copernicus data for the snapshots carried out in Aveiro in autumn.

The mean SPL values depicted in Figure 5.20 are presented in Table 11.

Table 11: Mean SPL values for each frequency in every hydrophone location, using Copernicus data.

	H3	H2	H1
63Hz	74,8	69,7	68,6
125Hz	71,5	72,2	68,0
250Hz	75,6	70,9	67,7
500Hz	70,8	63,0	59,8
2kHz	73,6	63,7	58,1
10kHz	68,6	63,5	57,1

5.2.4 Simulation with CTD data: Sound Pressure Level

The SPL outcomes derived from CTD information are depicted in Figure 5.21. The results range from 52,8 to 76,6 $dB\ re\ 1\mu Pa$, and the mean value is recorded as 66,8 $dB\ re\ 1\mu Pa$.

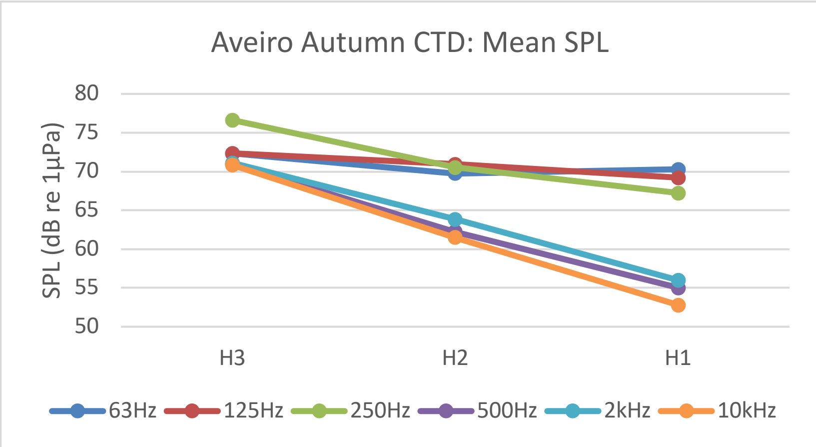

Figure 5.21: Mean sound pressure level graph for the three projections, each point representing a frequency with CTD data for the snapshots carried out in Aveiro in autumn.

When comparing the two simulations, it was observed that the mean values were similar but slightly higher when Copernicus data was utilized. In both scenarios, there is a decrease in SPL as one moves away from the source. Table 12 represents the values of mean SPL illustrated in Figure 5.21.

Table 12: Mean SPL values for each frequency in every hydrophone location, using CTD data.

	H3	H2	H1
63Hz	72,4	69,7	70,3
125Hz	72,4	70,9	69,2
250Hz	76,6	70,5	67,2
500Hz	71,0	62,2	55,0
2kHz	71,1	63,9	56,0
10kHz	70,8	61,5	52,8

5.3 1º Snapshot: Algarve Spring

On May 21st, 2021, the initial recording was conducted in Algarve using three hydrophones. The process is illustrated in Figure 5.22, with a total of three projections made at distances of $100\ m$, $250\ m$, and $500\ m$.

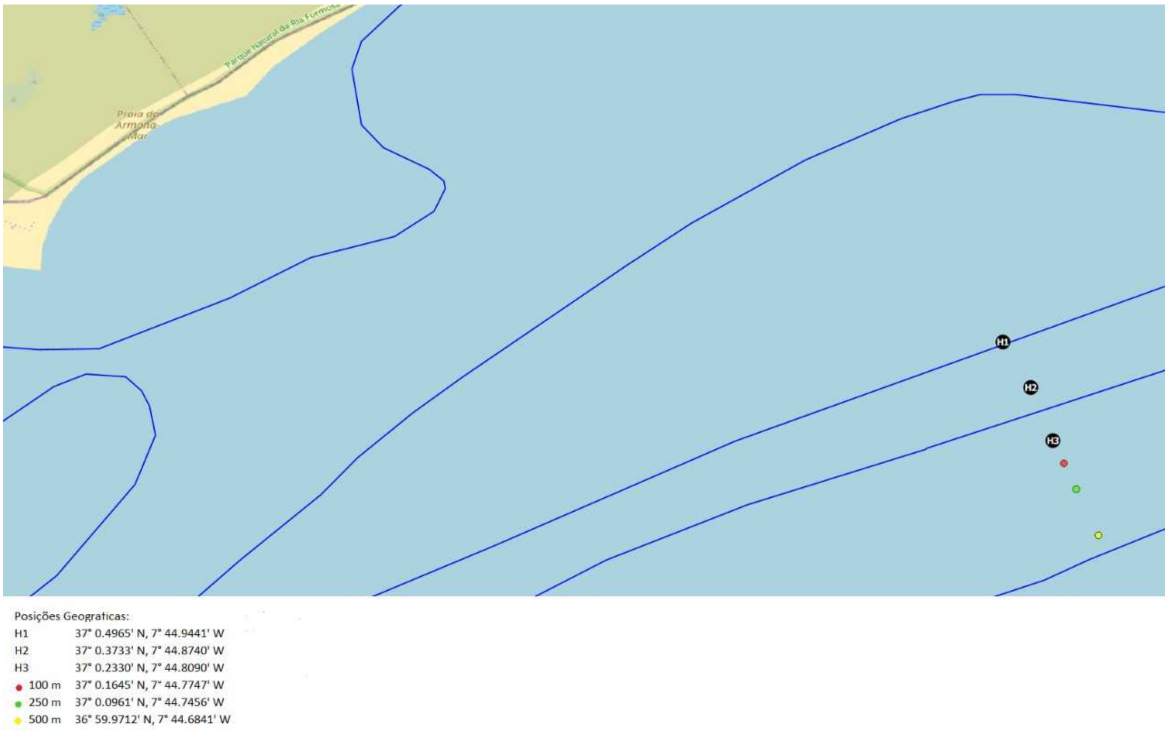

Figure 5.22: Configuration of the hydrophones and receptors for the first Algarve campaign.

By utilizing Equation 5.1 and considering the temperature, salinity, and depth profiles obtained from Copernicus data, sound speed profiles were generated. The results are shown in Figure 5.23 and were used for simulating projections at depths of $100\ m, 250\ m, and\ 500\ m$. Since the spatial resolution of the database only provides data for a single point, only one profile was used for the simulations.

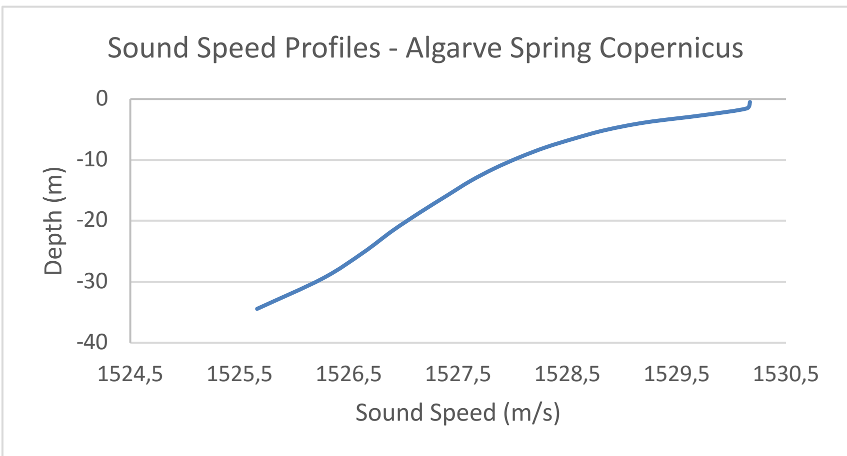

Figure 5.23: Average sound velocity (m/s) profile, for the snapshots carried out in Algarve in spring using Copernicus data.

5.3.1 Simulation with Copernicus data: Transmission Loss

Using the same approach as the Aveiro campaign, TL calculations were performed, and the results are depicted in Figure 5.24. The average TL value is $53{,}8\ dB$, with individual results ranging from $48{,}7\ dB$ to $60{,}9\ dB$.

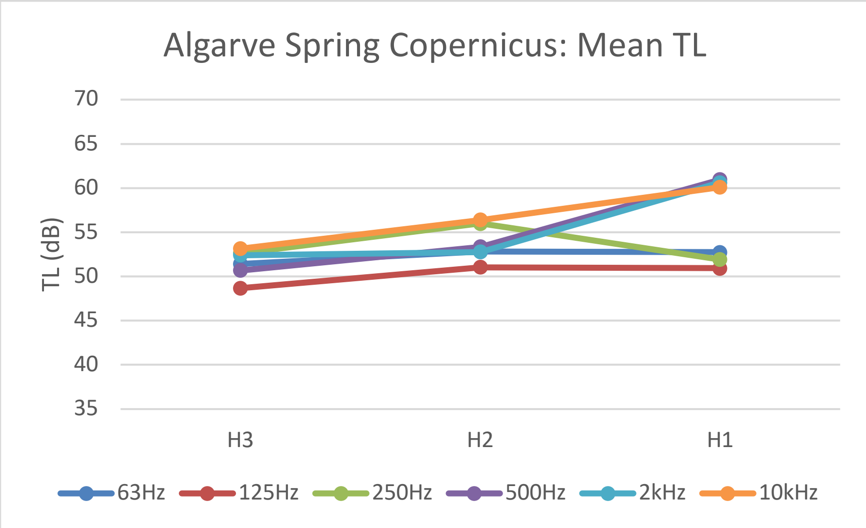

Figure 5.24: Mean transmission loss profile for the three projections, each point representing a frequency with Copernicus data for the snapshots carried out in Algarve in spring.

As the distance from the audio source increases, the TL also increases. When analyzing TL values specific to each frequency, it can be observed that they are most similar in the two hydrophones closest to the source location. Table 13 displays the mean TL values depicted in Figure 5.24.

Table 13: Mean TL values for each frequency in every hydrophone location, using Copernicus data.

	H3	H2	H1
63Hz	51,4	52,8	52,7
125Hz	48,7	51,0	50,9
250Hz	52,6	56,0	51,9
500Hz	50,7	53,4	61,0
2kHz	52,4	52,8	60,6
10kHz	53,1	56,4	60,1

5.3.2 Simulation with CTD data: Transmission Loss

The sound speed profiles were established using the CTD information collected during the expedition. For the projection at $500\ m$, all six profiles were considered. In the simulation for the projection at $100\ m$, depths up to $520\ m$ were included to incorporate all the profiles, while for the projection at $250\ m$, only depths up to $800\ m$ were used.

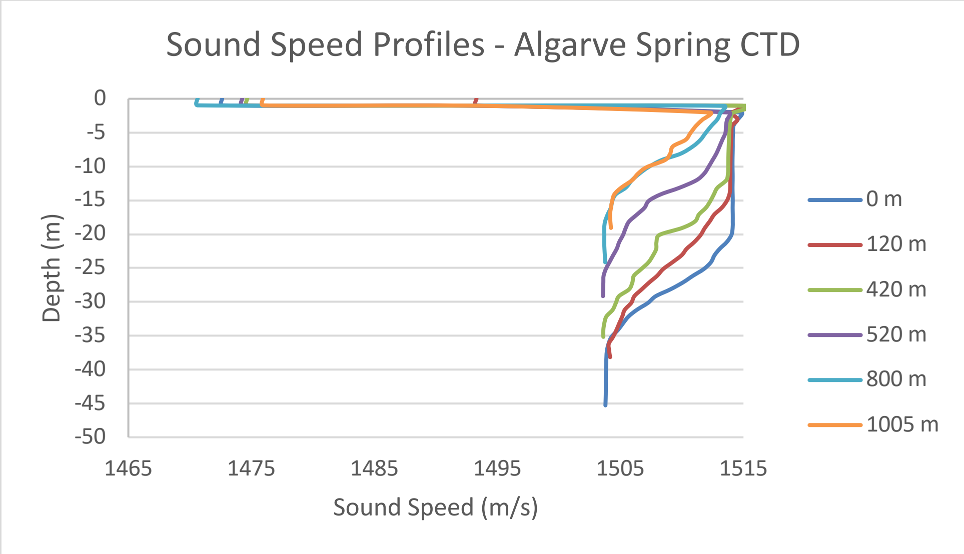

Figure 5.25: Sound speed profiles calculated from the CTD data.

Figure 5.26 depicts the TL calculated using CTD data. The average TL value across all frequencies is 53,4 dB, with a minimum of 35,5 dB and a maximum of 67,8 dB. Upon analyzing the frequency-based results in this experiment, it becomes evident that TL values are higher at high frequencies. While both simulations produce similar average results, incorporating CTD data leads to a wider range of TL measurements.

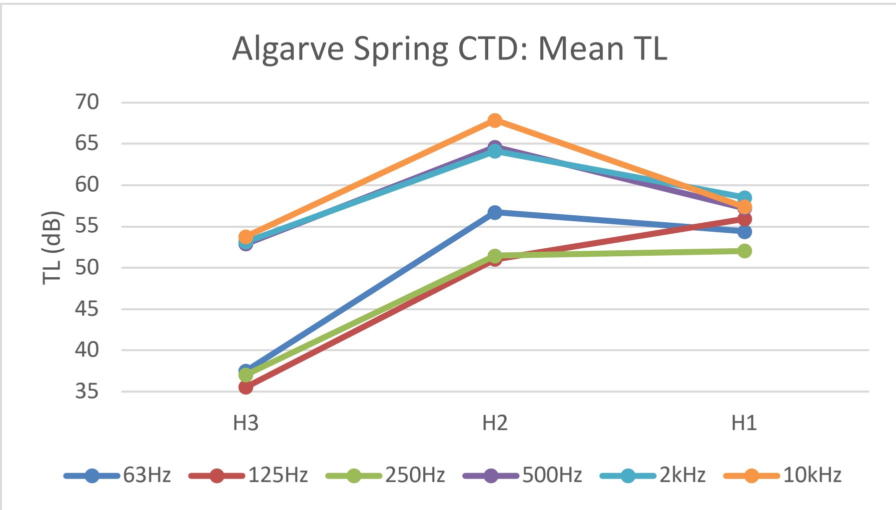

Figure 5.26: Mean transmission loss profile for the three projections, each point representing a frequency with CTD data for the snapshots carried out in Algarve in spring.

In Table 14 are represented the values of mean TL illustrated in Figure 5.26.

Table 14: Mean TL values for each frequency in every hydrophone location, using CTD data.

	H3	H2	H1
63Hz	37,5	56,7	54,4
125Hz	35,5	51,0	55,9

250Hz	37,0	51,5	52,0
500Hz	52,9	64,6	57,2
2kHz	53,1	64,1	58,5
10kHz	53,8	67,9	57,4

5.3.3 Simulation with Copernicus data: Sound Pressure Level

Using formula 5.2 and following the approach outlined in section 5.1.3, the SPL values were calculated for simulations using Copernicus data (Figure 5.27). As the distance from the source increases, there is a decrease in SPL, which ranges between 49,5 and 73,1 $dB\ re\ 1\mu Pa$. When located near the source (H3), the higher acoustic pressure results in elevated SPL values, while greater distances lead to diminishing acoustic pressure levels and subsequently lower SPL readings.

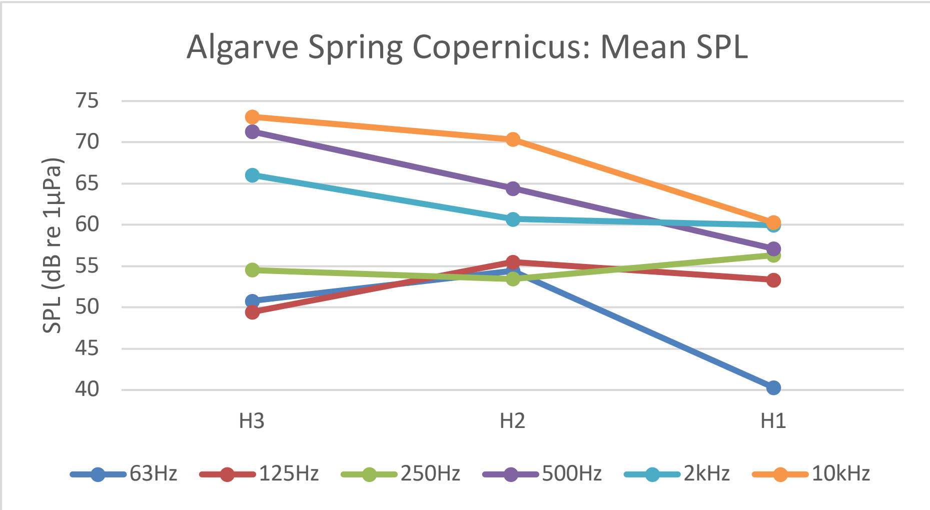

Figure 5.27: Mean sound pressure level for the three projections in Algarve during spring, with each data point representing a frequency and sourced from the Copernicus data of the snapshots.

The values of average SPL shown in Figure 5.27 are presented in Table 15.

Table 15: Mean SPL values for each frequency in every hydrophone location, using Copernicus data.

	H3	H2	H1
63Hz	50,8	54,4	40,3
125Hz	49,5	55,5	53,3
250Hz	54,5	53,4	56,3
500Hz	71,3	64,4	57,1
2kHz	66,0	60,7	60,0
10kHz	73,1	70,3	60,3

5.3.4 Simulation with CTD data: Sound Pressure Level

The SPL derived from CTD data is depicted in Figure 5.28. As previously noted, the SPL decreases as the distance from the source increases. The lowest SPL value recorded is

40,3 $dB\ re\ 1\mu Pa$, while the highest is 73,1 $dB\ re\ 1\mu Pa$. In both simulations, H3 hydrophone records the maximum values, while H1 hydrophone records the minimum values in terms of SPL readings.

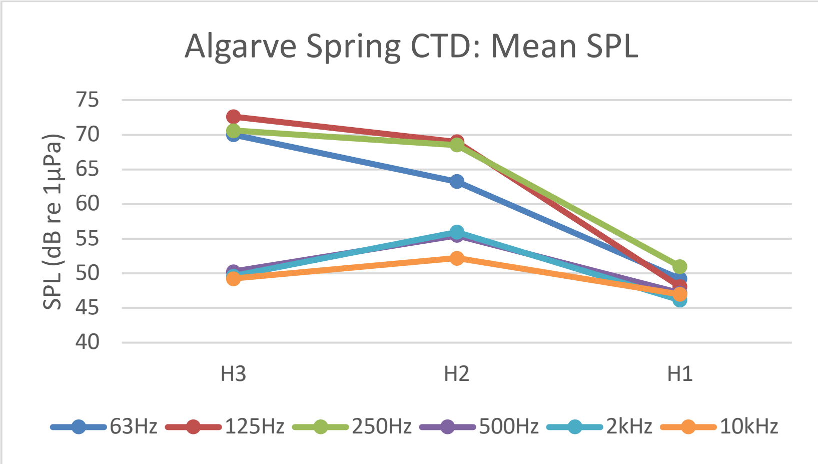

Figure 5.28: Mean SPL graph for the three projections, each point representing a frequency with CTD data for the snapshots carried out in Algarve in spring.

According to Copernicus data, the mean SPL value is $\mathbf{58,4\ dB\ re\ 1\mu Pa}$, whereas with CTD data, it is slightly lower at $\mathbf{56,4\ dB\ re\ 1\mu Pa}$. Although there are variations in the results when examining frequency-based SPL values using both datasets, their average values demonstrate a comparable pattern. The values of average SPL shown in Figure 5.27 are presented in Table 16.

Table 16: Mean SPL values for each frequency in every hydrophone location, using CTD data.

	H3	H2	H1
63Hz	72,3	69,7	70,3
125Hz	72,4	70,9	69,2
250Hz	76,6	70,5	67,2
500Hz	71,0	62,2	55,0
2kHz	71,1	63,9	56,0
10kHz	70,8	61,5	52,8

5.4 2º Snapshot: Algarve autumn

The second Algarve campaign was conducted on May 29th, 2021 with the aid of three hydrophones. Figure 5.29 represents the positions involved in the three measurements taken at distances of $100\ m, 250\ m, and\ 500\ m$, along with the locations of the hydrophones.

Figure 5.29: Configuration of the hydrophones and receptors for the second Algarve campaign.

5.4.1 Simulation for Transmission Loss

It was possible to determine sound speed profiles by using Equation 5.1 and taking into account the temperature, salinity, and depth profiles obtained from the Copernicus data. The results, which were used for simulating projections at depths of $100\ m, 250\ m, and\ 500\ m$, are displayed in Figure 5.30. Only one profile was used during the simulation process because the spatial resolution of the database only provides data for a single point.

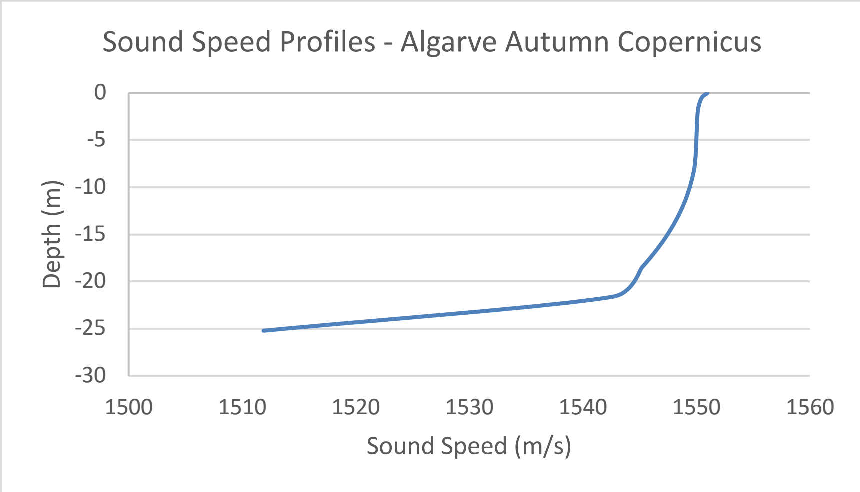

Figure 5.30: Average sound velocity (m/s) profile, for the snapshots carried out in Algarve in autumn.

The mean values of TL were calculated using the same methodology as the spring campaign, with the average value for all frequencies being 56,1 dB. When compared to the results from Figure 5.31, it demonstrates that the TL values range between 47,5 and 62,5 dB with less variation between them.

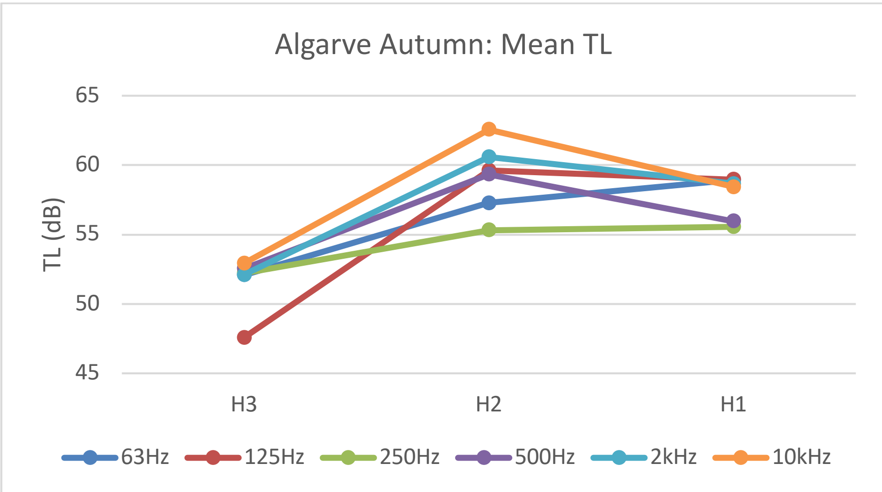

Figure 5.31: Mean transmission loss for the three projections in Algarve during Autumn, with each data point representing a frequency and sourced from the Copernicus data of the snapshots.

In Table 17 are represented the values of mean TL illustrated in Figure 5.31.

Table 17: Mean TL values for each frequency in every hydrophone location, using Copernicus data.

	H3	H2	H1
63Hz	52,1	57,3	58,9
125Hz	47,6	59,6	59,0
250Hz	52,2	55,3	55,6
500Hz	52,5	59,3	56,0
2kHz	52,1	60,6	58,7
10kHz	52,9	62,6	58,4

5.4.2 Simulation for Sound Pressure Levels

The mean SPL values were calculated using the same methodology as the spring campaign, with the average value coming out to $64{,}1\ dB\ re\ 1\mu Pa$. Figure 5.32 shows SPL values ranging from $57{,}4$ to $72{,}4\ dB\ re\ 1\mu Pa$, with less variation in the values compared to the results from the spring campaign.

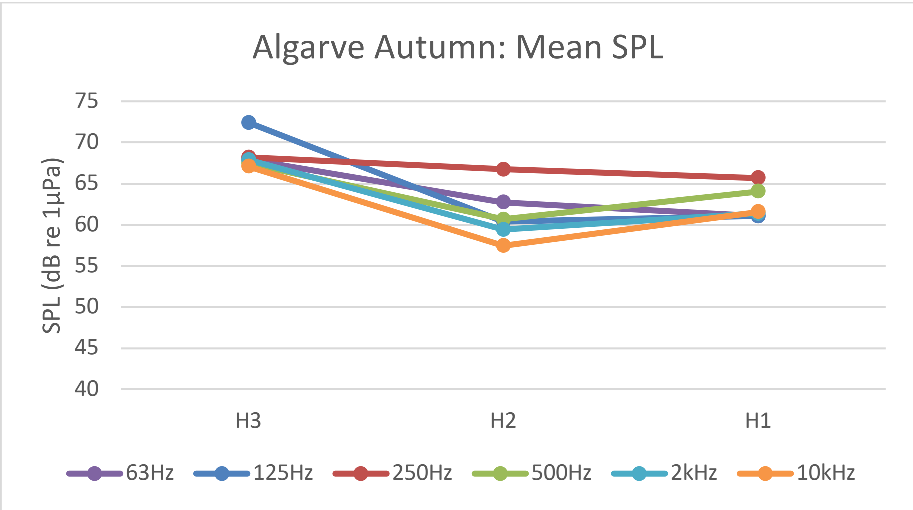

Figure 5.32: Mean SPL graph for the three projections, each point representing for the snapshots carried out in Algarve in autumn.

In this campaign, the H3 hydrophone records the highest values, while the H2 hydrophone records the lowest. When comparing the two campaigns, the SPL values are higher in the autumn, as evidenced by the higher average value and the average SPL graphs. Table 18 lists the average SPL values that are displayed in Figure 5.32.

Table 18: Mean SPL values for each frequency in every hydrophone location, using Copernicus data.

	H3	H2	H1
63Hz	67,9	62,7	61,1
125Hz	72,4	60,4	61,0
250Hz	68,2	66,8	65,7
500Hz	67,5	60,7	64,0
2kHz	67,9	59,4	61,4
10kHz	67,1	57,4	61,6

6 CONCLUSIONS

This report focuses on meeting the specific requirements and objectives of the project, which involve the use of modeling tools to study sound propagation in the marine environment. It provides a comprehensive presentation of the results derived from applying numerical models to the four campaigns conducted in Aveiro (during Spring and Autumn) and Algarve (also during Spring and Autumn). Furthermore, the report includes a comparative analysis of these results in relation to the data obtained through the use of hydrophones.

The analysis of the four campaigns conducted in Aveiro and Algarve yielded several key findings from the simulations:

- Sound Transmission Loss (TL): The TL values consistently increased with distance from the audio source in all campaigns, indicating a decrease in sound intensity as it propagated through water.
- Frequency Dependency: The simulations revealed variations in TL values across different frequency ranges. Higher frequencies generally exhibited higher TL values compared to lower frequencies. This frequency dependency is important for understanding the potential impact of underwater sound on marine ecosystems.
- Similarity between Simulations: Despite using different datasets (Copernicus and CTD data), the simulations exhibited similar trends and average values for TL and SPL. This suggests that both data sources can provide reliable information for modeling underwater sound propagation.
- Hydrophone Localization: The positioning of hydrophones influenced the recorded TL and SPL values. Hydrophones closer to the audio source recorded higher SPL values, indicating increased acoustic pressure in those areas.
- Data Resolution: The spatial resolution of the databases had an impact on the simulation results. Copernicus data, providing information for a single point, resulted in fewer profiles and a narrower range of TL and SPL values compared to CTD data, which incorporated multiple profiles.

Overall, these simulations emphasized the importance of considering environmental factors, such as temperature, salinity, and depth, when studying underwater sound propagation. The findings contribute to the assessment of underwater noise's potential impact on marine organisms and ecosystems, facilitating the development of effective mitigation strategies.

7 REFERENCES

Abraham, D. A. (2019). "*Underwater Acoustic Signal Processing – Modeling, Detection, and Estimation*." Springer Nature Switzerland. (ISBN 978-3-319-92981-1).

Ducan, A, J., & Maggi, A, L. (2006). "*A consistent, user friendly interface for running a variety of underwater acoustic propagation codes*". Proceedings of the First Australasian Acoustical Societies Conference, Christchurch, New Zealand, pp. 471–477. https://www.researchgate.net/publication/45813045_A_consistent_user_friendly_interface_for_running_a_variety_of_underwater_acoustic_propagation_codes.

Etter, P. C. (2018). "*Underwater Acoustic Modeling and Simulation – Fifth Edition*". Taylor & Francis Group. Boca Raton: CRC Press. (ISBN 978-1-1380-5492-9).

Küsel, E. T., & Siderius, M. (2019). "*Comparison of Propagation Models for the Characterization of Sound Pressure Fields*". *IEEE Journal of Oceanic Engineering*, vol. 44, no. 3, pp. 598-610. DOI: 10.1109/JOE.2018.2884107.

Leroy, C.C., Robinson, S.P., and Goldsmith, M.J. (2008). "*A new equation for the accurate calculation of sound speed in all oceans"*. J. Acoust. Soc. Amer., 124, 2774–82.

Maggi, A. L,. & Duncan, A. J. (2006). "*AcTUP v2.2 lα - Acoustic Toolbox User-interface & Postprocessor, Installation & User Guide*". Centre for Marine Science & Technology, University of Technology Curtin.

Porter, M.B. (2001). "*The Kraken Normal Mode Program - Draft*". SACLANT Undersea Research Center.

Porter, M.B. (2011). "*The Bellhop Manual and User's Guide: Preliminary Draft".* Heat, Light, and Sound Research, Inc La Jolla, CA, USA.

Sertlek, H. Ö., & Ainslie, M. A. (2013). "*Propagation loss models on selected scenarios from the Weston Memorial Workshop*". Proceedings of the 1st underwater acoustic conference (UAC), Corfu, Greece, pp 441–447. https://www.researchgate.net/publication/287782154_PROPAGATION_LOSS_MODEL_COMPARISONS_ON_SELECTED_SCENARIOS_FROM_THE_WESTON_MEMORIAL_WORKSHOP.

Thompson, S. R. (2009). "*Sound Propagation Considerations for a Deep-Ocean Acoustic Network*". Ph.D. Thesis, Naval Postgraduate School, Monterey, CA, USA.

8 ANNEX I. ACRONYMS

BELLHOP - Gaussian-Beam, Finite-Element, Range-Dependent Propagation Model

KRAKEN - Adiabatic/Coupled Normal Mode Model

OALIB - Ocean Acoustic Library

SPL - Sound Pressure Level

TL – Transmission Loss

underwater noise JUMP

Cofinanciado por:

REPÚBLICA PORTUGUESA MAR

fundoazul

underwater noise JUMP

Partners: